https://doi.org/10.1016/j.jpowsour.2022.232114

A high-performance H_2O_2-based fuel cell for air-free applications

Oladapo Christopher Esan[1], Xingyi Shi[1], Zhefei Pan[1], Yun Liu[1], Xiaoyu Huo[1], Liang An*[,1], T.S. Zhao*[,2]

[1]Department of Mechanical Engineering, The Hong Kong Polytechnic University, Hung Hom, Kowloon, Hong Kong SAR, China

[2]Department of Mechanical and Aerospace Engineering, The Hong Kong University of Science and Technology, Clear Water Bay, Kowloon, Hong Kong SAR, China

*Corresponding authors.

Email: liang.an@polyu.edu.hk (L. An)

Email: metzhao@ust.hk (T.S. Zhao)

Abstract

A newly introduced fuel cell which employs an electrically rechargeable liquid fuel (e-fuel) has piqued increasing research interest in recent years as it eliminates the need for catalyst materials at the anode. To further boost the performance of the e-fuel cell and realize its application in airtight environments, hydrogen peroxide (H_2O_2) is considered as an alternative oxidant instead of oxygen. Here, the operation and performance of a H_2O_2-based fuel cell is investigated. The novel e-fuel/H_2O_2 fuel cell displays a peak power density of 1456.0 mW cm^{-2} at 60 ℃, which is 70% higher than the use of oxygen (857.0 mW cm^{-2}). A maximum current density exceeding 3000 mA cm^{-2} is also achieved by the cell. Such impressive performance not only outclasses the e-fuel cell supplied with oxygen but also exceeds many liquid fuel cells that use H_2O_2 as oxidant. This therefore reveals the

capability of e-fuel/H_2O_2 fuel cell as a promising power source in airtight environments and high-power applications. The performance of the cell at various operating conditions including its discharge behaviour at constant currents are also investigated. This study thus offers stimulating insights for advanced investigations towards improving the design and operational characteristics of this H_2O_2-based fuel cell.

Keywords: Hydrogen peroxide; Fuel cell; E-fuel; Liquid fuel cell; Oxidant; Power density

1. Introduction

Depletion of resources and energy crisis in tandem with the increase in global population are undoubtedly some of the threatening challenges in our modern society.[1, 2] To significantly cut down the massive energy dependence on the limited and inefficient fossil fuels as well as their corresponding greenhouse gas emissions, the development and use of clean and renewable power sources are now of increasing importance and thus remain as one of the ultimate targets for researchers and scientists across the globe.[3-6] Over the years, fuel cell technology has emerged as an efficient and environmentally friendly energy conversion option as it converts the chemical energy available in fuel directly to electrical energy[7, 8]. Beginning with the use of hydrogen, a chemical energy carrier, hydrogen fuel cells received a broad array of applications, including the transport sector. However, the high-pressure requirement, safety and flammability issues, storage as well as transport difficulties of hydrogen seriously limit the continuous application and large-scale deployment of hydrogen fuel cells.[8-10] This therefore necessitated the needs to introduce and employ alternative fuels for the operation of fuel cell systems.

Due to the modularity and flexibility of utilization of fuel cells, a number of liquid fuels, including alcohols such as methanol and ethanol, have been employed to operate fuel cells. These liquid fuel cells have also been demonstrated to offer several benefits, including high energy density, high safety, and easy storage, in comparison to hydrogen fuel cells.[11, 12] Nevertheless, the high catalyst cost, fuel crossover, short durability, limited energy efficiency, and low power density associated with these direct liquid fuel cells later raised major concerns on the needs to utilize more efficient liquid fuels towards improving the cell performance. In response to this, the idea of using an electrically rechargeable liquid

fuel (e-fuel) was recently put forward[13] and is currently receiving an increasing research attention.[14, 15] Interestingly, both organic and inorganic materials were stated as prospective and suitable candidates to produce e-fuels. Subsequently, an e-fuel solution which contains vanadium ions dissolved in sulphuric acid was used to fuel the anode of a fuel cell and thereafter showcased its promising capabilities for running a fuel cell system.[16-18] Addressing the fuel issues prevalent in hydrogen and alcoholic fuel cells, the use of this e-fuel offers several advantages including the elimination of catalyst material at the anode, thereby reducing the fabrication cost of the cell. This particular e-fuel has therefore been demonstrated to possess excellent potential and fascinating properties to remain dominant over a long term in fuel cell applications.

Generally, an oxidant is required at the cathode of fuel cells. Gaseous oxygen or ambient air has been mostly employed for this purpose. However, their utility and performance are largely limited in air/oxygen-free environments and similar special conditions, such as space propulsion, underwater power systems, and applications requiring compact systems [19-22] As an alternative and a realistic oxidant, hydrogen peroxide has been demonstrated to be workable in fuel cells under the above-mentioned air-independent systems and for high power applications. In addition, the use of hydrogen peroxide provides several advantages in comparison with gaseous oxygen:[23-25] (1) significantly increases the theoretical voltage of the fuel cell, (2) offers low activation loss of reduction reaction due to two-electron transfer, (3) avoids water flooding issue and simplifies heat removal as a result of its intrinsic liquid phase, (4) offers higher current density due to its higher mass density compared to gas, and thus ultimately improves the performance of the fuel cell. Following

these intriguing advantages, hydrogen peroxide has been employed as oxidant in the operation of fuel cells.

Interestingly, the reduction reaction of hydrogen peroxide can occur in both acidic and alkaline media.[23] However, to achieve high fuel cell performance, the reduction reaction is mostly preferred in acidic media as a result of its inherently higher potential (1.78 V) compared to alkaline media (0.87 V).[23, 26] In addition, hydrogen peroxide is less stable in alkaline solution leading to its high decomposition rate.[27] On the other hand, the addition of sulfuric acid not only stabilizes the hydrogen peroxide solution but also enhances its electrochemical reduction.[23] While various fuels, including hydrazine[20] and ethylene glycol,[28] have been paired with hydrogen peroxide for fuel cell operations, sodium borohydride is the mostly used fuel in H_2O_2-based fuel cells with numerous studies, including the development of anode[29-32] and cathode electrocatalysts[33-35], and bipolar interface membrane electrode assembly[36, 37] with the aim to improve the performance of direct borohydride hydrogen peroxide fuel cells. However, the toxic nature and safety concerns regarding the hydrogen evolution of the borohydride solution and the undesired disparity between the pH environment of the alkaline anolyte and acidic catholyte[38, 39] have largely constrained the commercialization of direct borohydride hydrogen peroxide fuel cells.

Herein, the operation as well as the performance of an inherently compact H_2O_2-based e-fuel cell, as it combines an all-aqueous reactant and the superior advantages of both e-fuel (at the anode) and H_2O_2 (at the cathode), is experimentally examined. The hydrogen peroxide aqueous solution used at the cathode is, however, directly acidified using sulfuric

acid. The operation principle of this H2O2-based cell system, schematically presented in **Fig. 1**, is simply described below:

At the anode, the e-fuel is oxidized as follows:[40]

$$V^{2+} \rightarrow V^{3+} + e^{-} \qquad E_a = -0.26\,V \text{ vs. SHE} \qquad (1)$$

At the cathode, the reduction reaction of the hydrogen peroxide is as follows:[41]

$$H_2O_2 + 2H^{+} + 2e^{-} \rightarrow 2H_2O \qquad E_c = 1.78\,V \text{ vs. SHE} \qquad (2)$$

The overall reaction of the e-fuel/hydrogen peroxide cell is:

$$2V^{2+} + H_2O_2 + 2H^{+} \rightarrow 2V^{3+} + 2H_2O \qquad E_0 = 2.04\,V \qquad (3)$$

The experimental investigation of this novel e-fuel/hydrogen peroxide fuel cell produced a peak power density of 1456.0 mW cm^{-2} at 60 ℃, which is 70% higher than the use of oxygen (857.0 mW cm^{-2})[16], and also indicates a maximum current density exceeding 3000 mA cm^{-2}. Such impressive performance not only outshines the e-fuel cells receiving oxygen as oxidant, but also exceeds many of the regular direct liquid fuel cells whose oxidant is H2O2. This therefore reveals the capability of this e-fuel/hydrogen peroxide fuel cell as a promising power generation system in airtight environments and high-power applications. We further investigated the performance of the cell at various operating conditions including varying hydrogen peroxide concentration, sulfuric acid concentration, vanadium ion concentration, operating cell temperature, Nafion membrane thicknesses, and its constant-current discharge characteristics. The details of the experiment and the various results obtained from the investigations are discussed in subsequent sections.

2. Experimental details

2.1 Membrane electrode assembly

For the membrane electrode assembly, a catalyst-free graphite-felt electrode having a surface area of 4.0 cm^2 and treated by heating for five hours in the air while subjected to a temperature of 500℃ was used as the anode. A pretreated Nafion membrane, adopting the preparation method as reported in detail elsewhere,[42] of size 9.0 cm^2 was used for the experiment. A Pt/C coated carbon paper of 0.50 mg cm^{-2} loading produced by simply following the procedure used in one of our previous studies[43] was used as the cathode. Thereafter, these three aforementioned materials were assembled such that the Nafion membrane was properly placed in between the anode and the cathode to achieve the membrane electrode assembly.

2.2 Preparation of electrolytes

The anolyte, known as e-fuel, which fuels the anode was prepared as follows. $VOSO_4$ powder was first dissolved in H_2SO_4, the resulting solution was thereafter subjected to a charging process in a classic flow cell as described in an earlier study.[44] The catholyte, which is mostly referred to as oxidant in this study, is also an aqueous solution simply prepared by mixing sulfuric acid solution and hydrogen peroxide. After the preparation of both solutions, a 40.0 mL of both anolyte and catholyte was released into separate tanks for storage and in readiness for the cell operation.

2.3 Fuel cell set-up and instruments

The devices set-up for this experimental study is presented in **Fig. 2**. A peristaltic pump was assigned to each side of the cell to circulate the electrolytes through the cell. A temperature controller device (Anthone Electronic Co. Ltd., China) which has two heating

rods was later inserted, each for heating the anode and cathode side of the cell, and thermocouples for monitoring the temperature of the cell was also employed during the cell operation. The various experimental tests reported in this study were performed and recorded using a fuel cell testing system (Neware Technology Limited, China).

3. Results and discussion

3.1 General cell performance

The general performance of this H_2O_2-based fuel cell is presented in this section. The anolyte delivered into the cell during its operation is composed of 1.5 M V^{2+} in 4.0 M H_2SO_4 while the catholyte is a combination of 4.0 M H_2O_2 in 1.0 M H_2SO_4. Both anolyte and catholyte are pumped and circulated through the cell at a flow rate of 50.0 mL min^{-1}. The operating temperature of the cell is set at 60 ℃. Under such an operating condition, the cell achieved a peak power density of 1456.0 mW cm^{-2} and an open circuit voltage of 1.09 V as shown in **Fig. 3a**. The peak power density of this H_2O_2-based fuel cell demonstrates an impressive improvement in comparison to previous studies where oxygen/air are employed as oxidant in the demonstration of the e-fuel cell at 60 ℃ as presented in **Table S1**. The considerable performance enhancement can be majorly attributed to the several benefits, including higher theoretical voltage and lower cathode overpotential, of utilizing hydrogen peroxide as oxidant in the fuel cells. In comparison to direct liquid fuel cells that also employed hydrogen peroxide as oxidant, the performance of this H_2O_2-based e-fuel cell also substantially outperforms them all as presented in **Fig. 3b** and **Table S2**. For instance, a hydrazine/hydrogen peroxide fuel cell demonstrated at 60 ℃ could only achieved a peak power density of 780 mW cm^{-2},[20] which is about half of the peak power density attained by the H_2O_2-based fuel cell in this study. Even at a higher

operating temperature (80 ℃), the peak power density exhibited by the hydrazine/hydrogen peroxide fuel cell is 1020 mW cm^{-2} which is still lower than that of the e-fuel/hydrogen peroxide fuel cell. The widely studied direct borohydride/ hydrogen peroxide fuel cell demonstrated at 70 ℃ has been reported to achieve a peak power density of 890 mW cm^{-2} after introducing bipolar interface membrane electrode assembly.[45] In another research group, the direct borohydride fuel cell with hydrogen peroxide as oxidant exhibited a peak power density of 685 mW cm^{-2} at an operating cell temperature of 60 ℃.[46] Elsewhere, the direct borohydride/hydrogen peroxide fuel cell demonstrated similar performance at 60 ℃ to yield a peak power density of 680 mW cm^{-2}.[47] To the best of our knowledge, the peak power densities achieved by other fuel cells that employed hydrogen peroxide as oxidant all fall below 700 mW cm^{-2}, which further justify the superiority of this e-fuel/hydrogen peroxide fuel cell. Regarding open circuit voltage, the result achieved from this H_2O_2-based fuel cell is not only lower compared to when the cell was fed with oxygen at the cathode, but also lesser than its theoretical voltage. The drop in voltage can be ascribed to the decomposition of the hydrogen peroxide to produce oxygen at the cathode which in turn decreases the cathode potential.[41, 48] Moreover, the crossover of reactants from both sides of the cell, as both reactants are in liquid phase and can penetrate the Nafion membrane, can also reduce the open circuit voltage.[49] In particular, the crossover of the e-fuel to the cathode can cause large loss in the cathode potential as a result of mixed potential. While these issues are suggested to be addressed in future studies to increase the open circuit voltage, the impressive peak power density demonstrated by this e-fuel/hydrogen peroxide fuel cell positions it as a promising power generation system for air-free and high-power applications.

3.2 Effect of hydrogen peroxide concentration

Concentration is generally considered to be of significant influence on the rate of decomposition of hydrogen peroxide. Hence the effect of hydrogen peroxide concentration on the performance of this fuel cell is examined in this section. Here, various hydrogen peroxide concentrations varying from 1.0 to 6.0 M are considered with the concentration of the sulfuric acid set as 1.0 M for the oxidant at the cathode while the e-fuel solution at the anode is composed of 1.5 M V^{2+} in 4.0 M H_2SO_4. **Fig. 4**. displays the cell polarization and power density curves obtained from the investigations at an operating temperature of 60 ℃. As it can be seen, an upgrade in the performance of the cell is achieved all through the current density range when the hydrogen peroxide concentration is first increased from 1.0 M to 2.0 M. With an increase in the hydrogen peroxide concentration to 4.0 M, the cell performance was not only further enhanced but also displayed the highest performance. The commensurate increase in the cell performance with increase in the hydrogen peroxide concentration is majorly due to the enhanced mass transport of the reactive species at the cathode which consequently reduces concentration polarization loss and further improves the cell performance.[43, 50] A further increase in the hydrogen peroxide concentration to 6.0 M, however, decreases the cell performance below that of 4.0 M at all the current density region. The general decrease in the performance of the cell when the hydrogen peroxide concentration was increased to 6.0 M can be said to be from the competitive adsorption that happens between H_2O_2 and H^+ on the reactive spots in the cathode as a result of redundant H_2O_2.[51, 52] This therefore facilitates the undesirable concentration loss of H^+ and also heightens the internal resistance within the cell. In comparison to concentration at 2.0 M, the obtained cell voltage at the use of 6.0 M is also seen to fall below that of 2.0 M at

the low current density region and later increases above that of 2.0 M at higher current density. At low current density, the reduced cell voltage can be attributed to higher crossover rate of hydrogen peroxide to the anode as the membrane is permeable to hydrogen peroxide.[41, 53] The hydrogen peroxide that crossed over to the anode can react with the e-fuel and result to mixed potential at the anode which could raise the anode overpotential and hence decrease the cell voltage. At higher current density range, the reduced concentration loss as a result of high hydrogen peroxide concentration could be considered to have compensated for the mixed potential at the anode and thus only upgrade the cell performance above that of hydrogen peroxide concentration at 1.0 and 2.0 M but not that of 4.0 M. Overall, increasing the hydrogen peroxide concentration to 6.0 M is not beneficial to the cell voltage and its general performance, which therefore position an hydrogen peroxide concentration of 4.0 M as the optimal value to yield the best performance for the operation of this fuel cell.

3.3 Effect of sulfuric acid concentration

In this study, the hydrogen peroxide used at the cathode is directly acidified using sulfuric acid. As initially stated, the high potential of the reduction of hydrogen peroxide makes an acidic solution the more preferred media.[23] The addition of sulfuric acid to the hydrogen peroxide has also been reported to not only stabilizes the hydrogen peroxide but also enhances its electroreduction.[54] The concentration of the sulfuric acid added to the hydrogen peroxide aqueous solution would definitely influence the properties of the oxidant at the cathode and thus the overall performance of the cell. We therefore investigate the influence of the sulfuric acid concentration on the cell performance in this section. Here, the e-fuel is composed of 1.5 M V^{2+} in 4.0 M H_2SO_4 while 4.0 M H_2O_2 with varying

sulfuric acid concentrations from 0 to 3.0 M are used as the oxidant. The cell polarization and power density curves derived from this investigation at an operating temperature of 60 ℃ are presented in **Fig. 5**. At first, the cell was tested using a pure hydrogen peroxide solution, without adding sulfuric acid, as oxidant. It can be seen that the cell performance obtained is very low with a peak power density slightly above 400 mW cm^{-2}. With the addition of 1.0 M H_2SO_4 to the hydrogen peroxide solution as the catholyte, the peak power density is seen to dramatically increase and exhibit the highest performance of the cell. The explanation for this is that the presence of sulfuric acid results in higher concentration of H^+ at the cathode and also enhances its transport to the active sites in the catalyst layer, thereby accelerating the reduction reaction of the hydrogen peroxide.[51] Following this, the kinetic loss of the reduction reaction at cathode is reduced while the cathode potential and cell performance are improved. Afterwards, as the sulfuric acid concentration was further increased to 2.0 and 3.0 M, it can be seen that higher concentration of sulfuric acid does not offer improvement to the cell performance but rather a decrease throughout the whole current density region. The decrease in the cell voltage and power density with increase in the concentration of sulfuric acid can be attributed to the blocking of the active sites by the excessive sulfuric acid which in turn leads to insufficient presence of H_2O_2 in the catalyst layer leading to its concentration loss at the cathode thereby degrading the cell performance.[41, 51] In addition, higher concentration of sulfuric acid increases the viscosity of the catholyte which also impedes the transport of the reactants and in turn increases ohmic loss and degrade the cell performance.[52] The fuel cell therefore has its best performance when the concentration of the sulfuric acid employed acidify the hydrogen peroxide is 1.0 M.

3.4 Effect of vanadium ion concentration

The effect of vanadium ion concentrations on the cell performance was also explored. In this case, the concentration of the sulfuric acid in the anolyte was maintained at 4.0 M while various vanadium ion concentration of 0.1, 0.5, 1.0, and 1.5 M were used. The composition of the solution pumped into the cathode is 4.0 M H_2O_2 in 1.0 M H_2SO_4. The various polarization and power density curves obtained from this particular test at an operating temperature of 60 ℃ are shown in **Fig. 6**. As it can be viewed, the open circuit voltage, peak power density, and maximum current density of the cell significantly improve all through the current density range when the vanadium ion concentration was increased from 0.1 M to 1.5 M. In more details, with the first increase of the vanadium ion concentration from 0.1 M to 0.5 M, the open circuit voltage, peak power density, and maximum current density of the cell is observed to increase from 0.75 V, 145.3 mW cm^{-2}, and 660 mA cm^{-2} to 0.89 V, 701.9 mW cm^{-2}, and 2550 mA cm^{-2}, respectively. With a further increase of the vanadium ion concentration to 1.0 M and 1.5 M, it can be seen that in addition to the improvement in the open circuit voltage and peak power density of the cell, the maximum current density of the cell apparently exceeds 3000 mA cm^{-2} in both cases. Nevertheless, the highest performance of the cell with a peak power density of 1456.0 mW cm^{-2} was achieved at a vanadium ion concentration of 1.5 M. The cell performance significantly improves with the increase of the vanadium ion concentration due to the increase in the amount and supply of the reactant to the active sites at the anode. This therefore enhances the mass transport of the reactant at the anode which beneficially lowers concentration loss.[17, 55] Moreover, the increase of the vanadium ion concentration boosts the reaction kinetics at the anode which in turn reduces activation loss and augments

the cell performance. However, it is undeniable that the increase of vanadium concentration would also increase the viscosity of the fuel and thereby limit the mass transport of the reactants and eventually deteriorate the cell performance.[56] Within the range tested in this study, however, a higher vanadium concentration up to 1.5 M produced a better performance.

3.5 Effect of Nafion membranes

Membrane is an indispensable element in fuel cell design which not only serves as a medium for ions transport between the two sides of the cell but also prevents reactants crossover[57, 58]. Nafion series have been mostly considered and adopted in the operation of fuel cells due to the excellent chemical stability in addition to the high proton conductivity of these membranes[59, 60]. A number of Nafion membranes – 117, 115, 212, and 211 are therefore incorporated into the setup of this cell. The effects of these membranes, particularly their thickness – 183.0, 127.0, 50.8, and 25.4 μm, respectively, on the performance of the cell at an operating temperature of 60 ℃ are examined and the results are depicted in **Fig. 7a**. It can be seen that the general performance of the cell increases with the decrease in the thickness of the membranes used in the cell operation. In terms of their peak power density, Nafion 117, 115, 212, and 211 membranes exhibit 615.13, 665.94, 1039.56, and 1456.0 mW cm^{-2}, respectively. With the use of Nafion 211, the thinnest membrane, the cell was able to achieve a peak power density of 1456.0 mW cm^{-2} which is more than twice the peak power density (615.13 mW cm^{-2}) achieved when the thickest membrane, Nafion 117, was employed in the cell. In addition, the maximum current density observed when the cell used the thin membranes (Nafion 212 and 211) is apparently beyond 3000 mA cm^{-2} while the maximum current density realized with the use

of thick membranes (Nafion 117 and 115) are lower at 2100 and 2325 mA cm^{-2}, respectively. The decrease in the cell performance as the membrane thickness increases can be explained by the higher internal resistance associated with thick membranes which often results in voltage loss.[61, 62] However, the thick membranes are considered to be more suitable to prevent the crisscross of reactants to avoid mixed potential.[59] In other words, the use of thinner membrane leads to species crossover and cause mixed potential which could reduce the cell voltage. As seen in **Fig. 7a**, the cell voltage achieved at the low current density range with the use of Nafion 211, the thinnest membrane, is initially lower than others which can be ascribed to the crossover reactants. The thicker membranes therefore attained better performance in the low current density region while the thinner membranes performed better at the high current densities. Overall, these findings suggest that the high internal resistance associated with thick membranes overrides the effects of species crossover on the cell performance to produce the best performance with the use of Nafion 211. This therefore justifies the use of thinner membranes, such as Nafion 211, for cell operations where high power density is of paramount importance.

3.6 Effect of operating temperature

Operating temperature is a crucial parameter that is generally taken into consideration during the design and demonstration of fuel cells. The operating temperature not only reflects the thermal range of the fuel cell and its various components but also reflects their thermal behaviour and thereby provides useful insights on their thermal management. Furthermore, the chemical decomposition of the hydrogen peroxide used as the oxidant in this fuel cell is highly influenced by temperature and considered to be alleviated at lower temperatures.[23] This section therefore examines the performance of this H2O2-based fuel

cell under various operating temperature. The outcome of the investigation as displayed in **Fig. 7b** clearly shows that both the cell voltage and power density increases in tandem with the operating temperature. Starting with the operation of the cell at room temperature, taken as 23 ℃, a peak power density as high as 1033.6 mW cm^{-2} was achieved. On increasing the cell temperature to 40 ℃, the peak power density of the cell rose by 12 % to reach 1157.6 mW cm^{-2}. The investigation of the cell performance at an operating temperature of 60 ℃ accomplished a peak power density of 1456.0 mW cm^{-2} which is about 26 % higher than that of 40 ℃. The corresponding upgrade in cell performance as the operating temperature was raised from 23 to 60 ℃ can be explained as follows. Increasing the cell temperature enhances the transport of the e-fuel at the anode and the delivery of hydrogen peroxide at the cathode to their electrochemical reactive spots and further increases product removal rates, which beneficially reduces concentration loss.[63, 64] In addition, activation loss of the cell is significantly lowered as the operating temperature of the cell increases due to the improvement in the electrochemical kinetics on both electrodes. Furthermore, an increase in the operating temperature boosts the conductivity of the membrane which thus lessen the undesired ohmic loss within the cell and ultimately improves the cell performance.[65, 66] However, it worth to mention that a further raise of the operating temperature from 60 ℃ to 80 ℃ could barely offer significant cell performance improvement as it can be seen in **Fig. 7b**. Such a high operating temperature speeds up the violent decomposition of hydrogen peroxide to oxygen, which consequently lowers the cathode potential.[41, 48] Moreover, the cell is predisposed to a high reactant crossover at higher temperatures resulting into a mixed potential which degrades the electrode potential

and thus deteriorates the cell performance.[63] Following this, 60 ℃ is considered as the optimal operating temperature suitable for the high performance of this cell.

3.7 Constant-current discharge behaviour

The purpose of the constant-current discharge test is to evaluate the performance of the fuel cell similar to its real-life applications. In this study, the constant current discharge test is conducted at 50, 100, and 200 mA cm^{-2} under an operating temperature of 60 ℃. Results from the constant-current discharge test are further used to calculate the Faradic, voltage, and energy efficiencies of the cell. As shown in **Fig. 8a,** it is clear that the voltage plateau and the discharge capacity of the cell increases with the constant current. This therefore produced voltage efficiency of 46.7%, 47.3%, and 47.3%, under the three different currents considered as shown in **Fig. 8b.** In addition, the discharge capacity of the cell under these three constant currents are 1.92, 6.67, and 12.5 Ah L^{-1}, respectively, which clearly increases with the constant currents. Such results thus demonstrate the increase of the constant discharge current could enable a better utilization of the reactants, where the energy efficiency of the cell, as shown in **Fig. 8b** is also seen to increase from 2.3 % to 14.7 % as the operating current is increased from 50 to 200 mA cm^{-2}. Even though, there is room for the improvement of the energy efficiency, this trend suggests that the cell has potential for higher energy efficiency when subjected to higher constant current. Furthermore, to ascertain the ability of this system for long-term operations, it has been refueled for 10 times while discharging at a constant current of 10 mA cm^{-2} under an operating temperature of 60 ℃ (**Fig. S1)** proving its good stability. However, it is worth to mention that, during the cell operation, the e-fuel and hydrogen peroxide could penetrate the membrane to the

opposite side leading to the corrosion of the electrodes which in turn degrade the cell performance and thus require careful attention.

4. Summary

This study presents the operation and performance of a high-performance H2O2-based fuel cell for application in air-tight environments. As an alternative oxidant, in place of gaseous oxygen or ambient air, hydrogen peroxide is used at the cathode side of an e-fuel cell. The results obtained from this experimental study show that the application of hydrogen peroxide as oxidant substantially bolsters the performance of the cell to achieve a peak power density of 1456.0 mW cm^{-2} at 60 ℃ and a maximum current density which exceeds 3000 mA cm^{-2}. This impressive performance not only outshines the e-fuel cell fed with oxygen as oxidant but also exceeds most of the regular direct liquid fuel cells that also employ hydrogen peroxide as oxidant. Further investigations reveals that the cell performance increases with hydrogen peroxide concentration till 4.0 M, above which the performance starts to drop Acidifying the hydrogen peroxide with sulfuric acid concentration of 1.0 M yields the best cell performance. As for the vanadium ion, increasing its concentration from 0.5 M to 1.5 M contributes to the improvement of the cell performance. An operating temperature of 60 ℃ is considered suitable for the operation and high performance of this cell. Nafion 211 is demonstrated as the most suitable membrane for the cell operations as high-power density is of paramount importance for aerospace propulsion and underwater power systems. It is worth to mention that the use lower Pt/C loading at the cathode during the cell fabrication to further reduce the cost of the cell is of great importance before achieving the commercialization of this system and it will be one of our major study directions in the future. This study thus provides

stimulating insights for future investigations towards improving the design and operating condition of this particular H2O2-based fuel cell for advanced operations and applications.

Acknowledgement

The research work presented here was fully supported by a grant received from the Research Grant Council of the Hong Kong Special Administrative Region, China (Project No. T23-601/17-R).

References

1. F. Ueckerdt, C. Bauer, A. Dirnaichner, J. Everall, R. Sacchi and G. Luderer, *Nature Climate Change*, 2021, **11**, 384-393.
2. B. Stolz, M. Held, G. Georges and K. Boulouchos, *Nature Energy*, 2022, 1-10.
3. M. Chen, Y. Zhang, G. Xing, S.-L. Chou and Y. Tang, *Energy & Environmental Science*, 2021, **14**, 3323-3351.
4. O. C. Esan, X. Shi, Z. Pan, X. Huo, L. An and T. Zhao, *Advanced Energy Materials*, 2020, **10**, 2000758.
5. H. Feng, D. Liu, Y. Zhang, X. Shi, O. C. Esan, Q. Li, R. Chen and L. An, *Advanced Energy Materials*, 2022, 2200469.
6. S. Chen, M. Zhang, P. Zou, B. Sun and S. Tao, *Energy & Environmental Science*, 2022.
7. A. Sajid, E. Pervaiz, H. Ali, T. Noor and M. M. Baig, *International Journal of Energy Research*, 2022, **46**, 6953-6988.
8. N. Shaari, S. K. Kamarudin, R. Bahru, S. H. Osman and N. A. I. Md Ishak, *International Journal of Energy Research*, 2021, **45**, 6644-6688.
9. D. A. Cullen, K. C. Neyerlin, R. K. Ahluwalia, R. Mukundan, K. L. More, R. L. Borup, A. Z. Weber, D. J. Myers and A. Kusoglu, *Nature energy*, 2021, **6**, 462-474.
10. K. Swider-Lyons and D. Deitz, *ECS Transactions*, 2016, **75**, 479.
11. V. S. Pinheiro, F. M. Souza, T. C. Gentil, A. N. Nascimento, L. S. Parreira, M. I. Sairre, B. L. Batista and M. C. Santos, *Journal of Alloys and Compounds*, 2022, **899**, 163361.
12. Y. Yang, X. Zhu, Q. Wang, D. Ye, R. Chen and Q. Liao, *Applied Thermal Engineering*, 2022, **203**, 117937.
13. H. Jiang, L. Wei, X. Fan, J. Xu, W. Shyy and T. Zhao, *J Science Bulletin*, 2019, **64**, 270-280.
14. X. Shi, X. Huo, O. C. Esan, Y. Ma, L. An and T. Zhao, *Journal of Power Sources*, 2021, **506**, 230198.
15. X. Shi, X. Huo, O. C. Esan, Y. Dai, L. An and T. Zhao, *ACS Applied Materials & Interfaces*, 2022, **14**, 18600-18606.
16. X. Shi, X. Huo, O. C. Esan, L. An and T. Zhao, *Applied Energy*, 2021, **297**, 117145.
17. X. Shi, Y. Dai, O. C. Esan, X. Huo, L. An and T. Zhao, *ACS Applied Materials & Interfaces*, 2021, **13**, 48795-48800.
18. O. C. Esan, X. Shi, Y. Dai, L. An and T. S. Zhao, *Applied Energy*, 2022, **311**, 118677.
19. S. Fukuzumi, Y.-M. Lee and W. Nam, *Chinese Journal of Catalysis*, 2021, **42**, 1241-1252.
20. S. J. Lao, H. Y. Qin, L. Q. Ye, B. H. Liu and Z. P. Li, *Journal of Power Sources*, 2010, **195**, 4135-4138.
21. T. H. Oh, *Aerospace Science and Technology*, 2016, **58**, 511-517.
22. N. Luo, G. Miley, K.-J. Kim, R. Burton and X. Huang, *Journal of Power Sources*, 2008, **185**, 685-690.
23. L. An, T. Zhao, X. Yan, X. Zhou and P. Tan, *Science Bulletin*, 2015, **60**, 55-64.
24. G. H. Miley, N. Luo, J. Mather, R. Burton, G. Hawkins, L. Gu, E. Byrd, R. Gimlin, P. J. Shrestha and G. Benavides, *Journal of Power Sources*, 2007, **165**, 509-516.

25. R. O. Stroman, G. S. Jackson, Y. Garsany and K. Swider-Lyons, *Journal of Power Sources*, 2014, **271**, 421-430.
26. X. Jing, D. Cao, Y. Liu, G. Wang, J. Yin, Q. Wen and Y. Gao, *Journal of electroanalytical chemistry*, 2011, **658**, 46-51.
27. A. Oshchepkov, A. Bonnefont, G. Maranzana, E. R. Savinova and M. Chatenet, *Current Opinion in Electrochemistry*, 2022, **32**, 100883.
28. Z. Pan, Z. Zhang, A. Tahir, O. C. Esan, X. Liu, H. Wang and L. An, *International Journal of Energy Research*, 2022, **46**, 13820-13831.
29. R. M. Hjelm, C. Lafforgue, R. W. Atkinson, Y. Garsany, R. O. Stroman, M. Chatenet and K. Swider-Lyons, *Journal of The Electrochemical Society*, 2019, **166**, F1218.
30. K. Swider-Lyons, R. M. Hjelm, Y. Garsany, C. Lafforgue and M. Chatenet, *Journal of The Electrochemical Society*, 2020, **167**, 164508.
31. R. M. E. Hjelm, Y. Garsany, R. W. Atkinson, R. O. N. Stroman, K. Swider-Lyons, C. Lafforgue and M. Chatenet, *ECS Transactions*, 2017, **80**, 1033.
32. P.-Y. Olu, N. Job and M. Chatenet, *Journal of Power Sources*, 2016, **327**, 235-257.
33. C. P. de León, F. Walsh, C. Patrissi, M. Medeiros, R. Bessette, R. Reeve, J. Lakeman, A. Rose and D. Browning, *Electrochemistry communications*, 2008, **10**, 1610-1613.
34. T. H. Oh, *Renewable Energy*, 2021, **163**, 930-938.
35. S. S. Yu, T. H. Lee and T. H. Oh, *Fuel*, 2022, **315**, 123151.
36. Z. Wang, J. Parrondo, C. He, S. Sankarasubramanian and V. Ramani, *Nature Energy*, 2019, **4**, 281-289.
37. C. G. Arges, V. Prabhakaran, L. Wang and V. Ramani, *International Journal of Hydrogen Energy*, 2014, **39**, 14312-14321.
38. Z. Wang, S. Sankarasubramanian and V. Ramani, *Current Opinion in Electrochemistry*, 2018, **12**, 240-245.
39. M. Chatenet, *Nature Energy*, 2019, **4**, 261-262.
40. O. C. Esan, X. Shi, X. Su, Y. Dai, L. An and T. Zhao, *Journal of Power Sources*, 2021, **501**, 230023.
41. Z. Pan, B. Huang and L. An, *International Journal of Energy Research*, 2019, **43**, 2583-2591.
42. B. Jiang, L. Wu, L. Yu, X. Qiu and J. Xi, *Journal of Membrane Science*, 2016, **510**, 18-26.
43. L. An and T. Zhao, *International journal of hydrogen energy*, 2011, **36**, 9994-9999.
44. H. Jiang, W. Shyy, M. Wu, L. Wei and T. Zhao, *Journal of Power Sources*, 2017, **365**, 34-42.
45. Z. Wang, S. Sankarasubramanian and V. Ramani, *Cell Reports Physical Science*, 2020, **1**, 100084.
46. J. Ma and Y. Sahai, *ECS Transactions*, 2012, **42**, 101.
47. G. H. Miley, R. Bernas, K.-J. Kim and N. Luo, *ECS Transactions*, 2009, **17**, 525.
48. Y. Li, Y. He and W. Yang, *Journal of Power Sources*, 2015, **278**, 569-573.
49. L. An, T. Zhao, R. Chen and Q. Wu, *Journal of power sources*, 2011, **196**, 6219-6222.
50. T. H. Oh, *Renewable Energy*, 2021, **178**, 1156-1164.
51. Z. Pan, Y. Bi and L. An, *Applied Energy*, 2019, **250**, 846-854.

52. Z. Pan, H. Zhuang, Y. Bi and L. An, *Journal of Power Sources*, 2019, **437**, 226944.
53. L. An, T. S. Zhao and J. B. Xu, *International Journal of Hydrogen Energy*, 2011, **36**, 13089-13095.
54. R. Raman and A. Shukla, *Journal of applied electrochemistry*, 2005, **35**, 1157-1161.
55. X. Shi, X. Huo, Y. Ma, Z. Pan and L. An, *Cell Reports Physical Science*, 2020, **1**, 100102.
56. Y. Zhao, L. Liu, X. Qiu and J. Xi, *Electrochimica Acta*, 2019, **303**, 21-31.
57. X. Shi, O. C. Esan, X. Huo, Y. Ma, Z. Pan, L. An and T. Zhao, *Progress in Energy and Combustion Science*, 2021, **85**, 100926.
58. X. Shi, Y. Bi, O. C. Esan and L. An, in *60 Years of the Loeb-Sourirajan Membrane*, Elsevier, 2022, pp. 155-175.
59. X. Shi, Y. Ma, X. Huo, O. C. Esan and L. An, *International Journal of Green Energy*, 2021, 1-7.
60. L. An and C. Jung, *Applied energy*, 2017, **205**, 1270-1282.
61. S. Won, K. Oh and H. Ju, *Electrochimica Acta*, 2015, **177**, 310-320.
62. W. Haijun, W. Cheng, L. Zhixiang and M. Zongqiang, *International journal of hydrogen energy*, 2010, **35**, 2648-2651.
63. Y. Li, H. Wu, Y. He, Y. Liu and L. Jin, *Journal of Power Sources*, 2015, **287**, 75-80.
64. A. Uzundurukan, E. S. Akça, Y. Budak and Y. Devrim, *Renewable Energy*, 2021, **172**, 1351-1364.
65. L. An, T. S. Zhao, L. Zeng and X. H. Yan, *International Journal of Hydrogen Energy*, 2014, **39**, 2320-2324.
66. L. An, T. Zhao, X. Zhou, L. Wei and X. Yan, *RSC Advances*, 2014, **4**, 65031-65034.

Figure captions

Fig. 1. The operation principle of the e-fuel/hydrogen peroxide fuel cell.

Fig. 2. Experimental set-up for the operation of the e-fuel/hydrogen peroxide fuel cell.

Fig. 3. Polarization and power density curves of the H_2O_2-based fuel cell and (b) Comparison of power density with data obtained from the open literature for direct liquid fuel cells that employed H_2O_2 as oxidant.

Fig. 4. Effect of hydrogen peroxide concentration on the cell performance.

Fig. 5. Effect of sulfuric acid concentration on the cell performance.

Fig. 6. Effect of vanadium ion concentration on the cell performance.

Fig. 7. (a) Effect of Nafion membranes on the cell performance and (b) Effect of operating temperature on the cell performance.

Fig. 8. (a) Constant-current discharge performances and (b) Efficiencies of the cell under three different current densities – 50, 100, and 200 mA cm^{-2}.

Figures

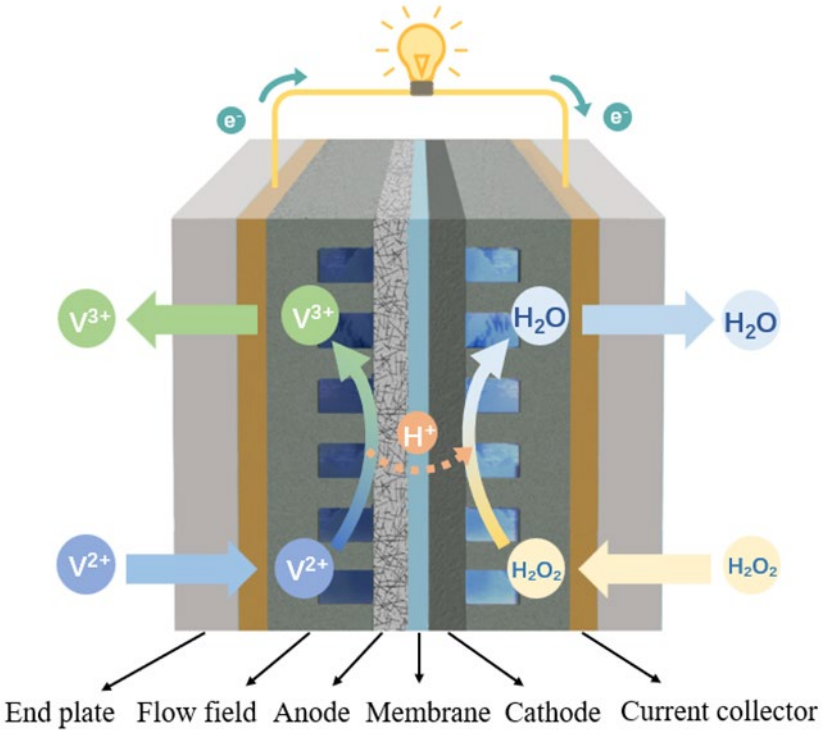

Fig. 1. The operation principle of the e-fuel/hydrogen peroxide fuel cell.

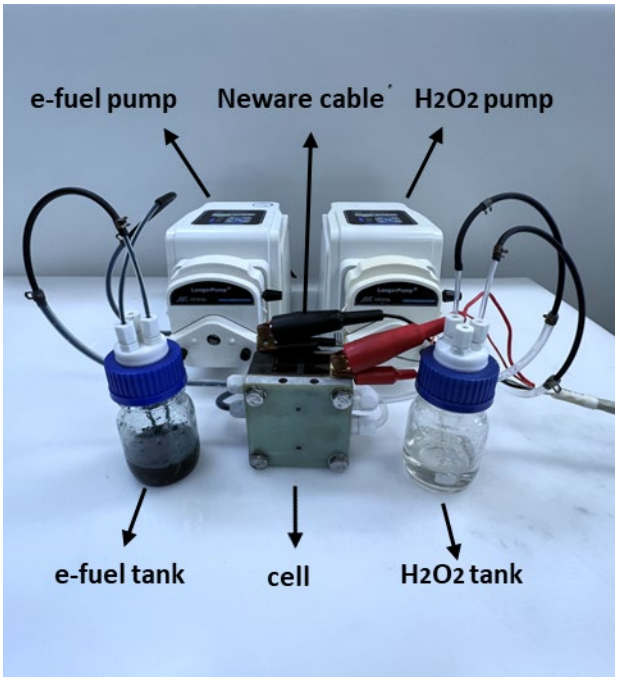

Fig. 2. Experimental set-up for the operation of the e-fuel/hydrogen peroxide fuel cell.

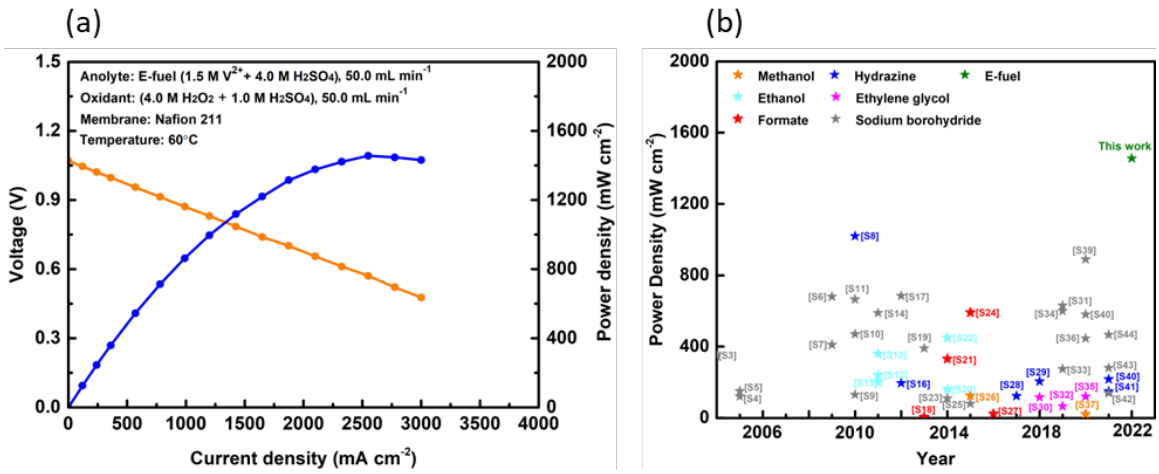

Fig. 3(a) Polarization and power density curves of the H2O2-based fuel cell and (b) Comparison of power density with data obtained from the open literature for direct liquid fuel cells that employed H2O2 as oxidant.

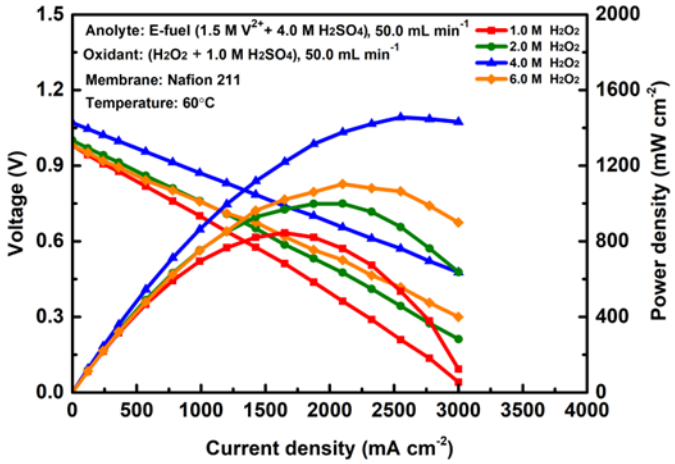

Fig. 4. Effect of hydrogen peroxide concentration on the cell performance.

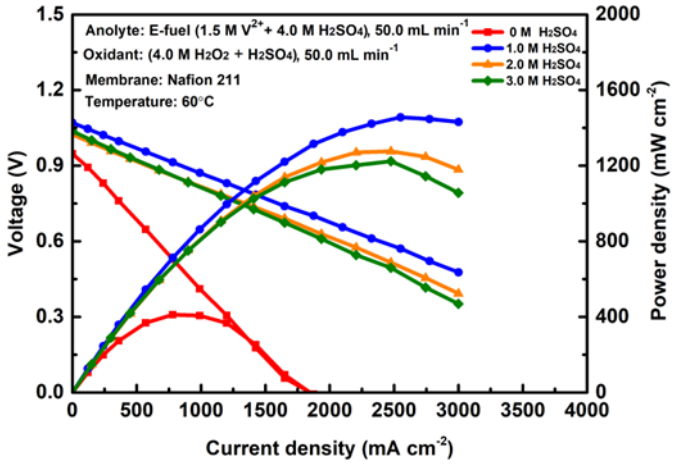

Fig. 5. Effect of sulfuric acid concentration on the cell performance.

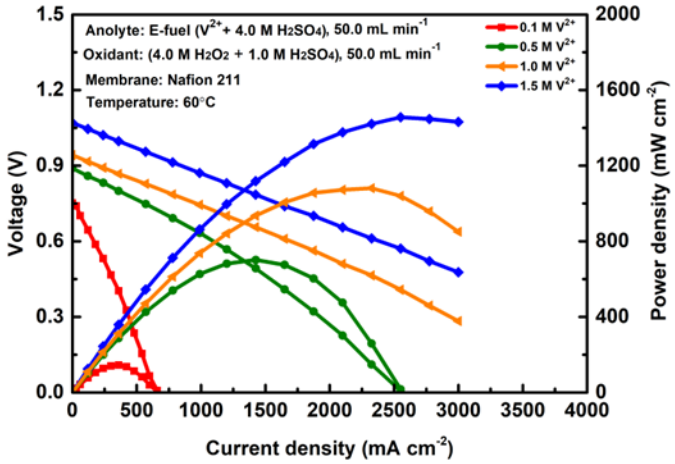

Fig. 6. Effect of vanadium ion concentration on the cell performance.

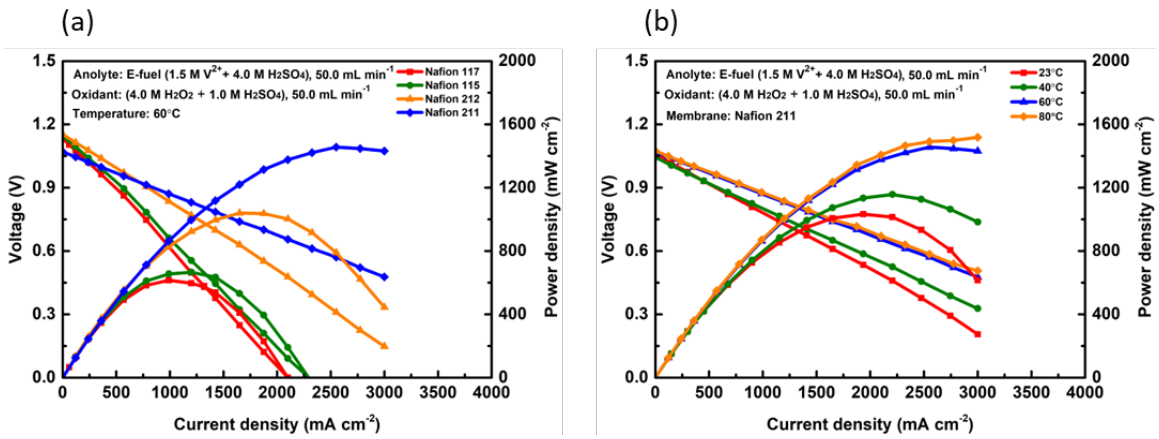

Fig. 7. (a) Effect of Nafion membranes on the cell performance and (b) Effect of operating temperature on the cell performance.

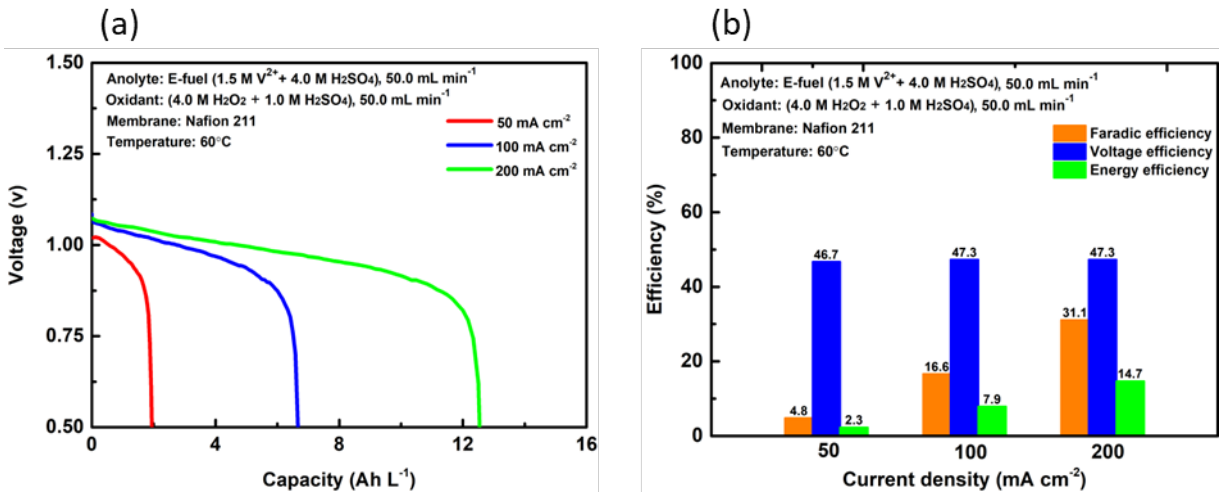

Fig. 8(a) Constant-current discharge performances and (b) Efficiencies of the cell under three different current densities – 50, 100, and 200 mA cm^{-2}.

Supplementary information

A high-performance H_2O_2-based fuel cell for air-free applications

Oladapo Christopher Esan[1], Xingyi Shi[1], Zhefei Pan[1], Yun Liu[1], Xiaoyu Huo[1], Liang An*[,1], T.S. Zhao*[,2]

[1]Department of Mechanical Engineering, The Hong Kong Polytechnic University, Hung Hom, Kowloon, Hong Kong SAR, China

[2]Department of Mechanical and Aerospace Engineering, The Hong Kong University of Science and Technology, Clear Water Bay, Kowloon, Hong Kong SAR, China

*Corresponding authors.

Email: liang.an@polyu.edu.hk (L. An)

Email: metzhao@ust.hk (T.S. Zhao)

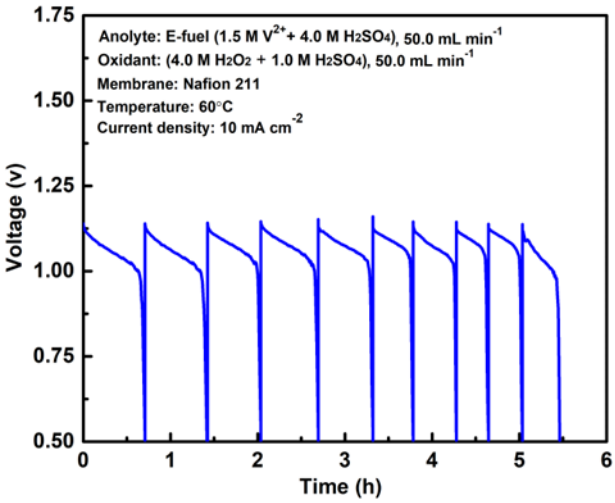

Fig. S1. Durability of the cell showing its discharging behavior after refueling for 10 times.

Table S1. Performance comparison with previous e-fuel cells using different oxidants.

Year	Fuel	Membrane	Oxidant	Temp. (℃)	Cathode catalyst (mg cm^{-2})	Peak power density (mW cm^{-2})	Ref.
2021	E-fuel	Nafion 117	Air	60	Pt/C (0.5)	199.5	[18]
2021	E-fuel	Nafion 211	Oxygen	60	Pt/C (4.0)	857.0	[16]
2022	E-fuel	Nafion 211	Hydrogen peroxide	60	Pt/C (0.5)	1456.0	This work

Table S2. Performance comparison of direct liquid fuel cells that employed hydrogen peroxide as oxidant.

Year	Fuel	Membrane	Temp (°C)	Cathode Catalyst (mg cm^{-2})	Peak power density (mW cm^{-2})	Ref.
2004	Sodium borohydride	Nafion 117	70	Pt/C (1.0)	350	67
2005	Sodium borohydride	Nafion 117	70	$PbSO_4$/C (8.0)	120	54
2005	Sodium borohydride	Nafion 117	70	Pt/C (1.0)	150	68
2009	Sodium borohydride	Nafion 112	60	Pd (0.1)	680	47
2009	Sodium borohydride	Nafion membrane	80	Pt/C (1.8)	410	69
2010	Hydrazine	Nafion 112	80	Au/C (1.0)	1020	20
2010	Sodium borohydride	Nafion 117	80	MnO_2 (4.0)	130	62
2010	Sodium borohydride	Nafion 117	22	Pt	470	70
2010	Sodium borohydride	Nafion 212	60	Pd (1.0)	665	71
2011	Ethanol	Nafion 117	60	PdNi/C (3.9)	240	72
2011	Ethanol	Nafion 211	60	Pt/C (4.0)	360	73
2011	Sodium borohydride	Nafion 117	70	Pd/C (1.0)	589	74
2011	Ethanol	Nafion 117	60	Au/C (1.2)	200	53
2012	Hydrazine	Nafion 115	80	Pt/C (0.1)	195	75
2012	Sodium borohydride	Chitosan hydrogel	60	Pd	685	46
2013	Formate	-	25	Pt/C (1.0)	4.9	76
2013	Sodium borohydride	Nafion 212	80	Nano porous gold leaves (0.12)	390	77
2014	Ethanol	A201	80	ACTA (1.0)	160	65
2014	Formate	Nafion 115	60	Pt/C (3.0)	331	48
2014	Ethanol	Nafion 117	60	-	450	66

Year	Fuel	Membrane	Temp (℃)	Cathode Catalyst (mg cm^{-2})	Peak power density (mW cm^{-2})	Ref.
2014	Sodium borohydride	Bipolar junction	70	Pt/C (1.0)	110	[37]
2015	Formate	Nafion 115	60	Pt/C (2.0)	591	[63]
2015	Sodium borohydride	Nafion 117	25	Pt/C (0.14)	79.9	[78]
2015	Methanol	Nafion 115	60	PB/CNT (20.0)	125	[79]
2016	Formate	A201	40	Pt/C (2.0)	23	[80]
2017	Hydrazine	Nafion 117	60	Au/C (1.0)	122.75	[81]
2018	Hydrazine	Nafion 117	60	Pt/C (0.5)	204.8	[82]
2018	Ethylene glycol	Nafion 212	80	Au/C (2.66)	115.3	[41]
2019	Sodium borohydride	Nafion 117	25	Pt/C (0.3)	275	[29]
2019	Ethylene glycol	Nafion 211	60	Au/C (2.66)	65.8	[51]
2019	Sodium borohydride	Bipolar junction	70	Pt/C (3.0)	630	[36]
2019	Sodium borohydride	Nafion HP	60	Pt/CB	~600	[83]
2020	Ethylene glycol	Nafion 211	60	Au/C (2.66)	120	[84]
2020	Sodium borohydride	Bipolar interface	70	Pt/C (1.0)	446	[85]
2020	Methanol	Nafion 115	85	PB (6.7)	20.5	[86]
2020	Sodium borohydride	Bipolar interface	25	Pt/C (3.0)	580	[87]
2020	Sodium borohydride	Bipolar interface	70	Pt/C (3.0)	890	[45]
2021	Hydrazine	Nafion 117	60	Pt/C (0.5)	216.71	[88]
2021	Hydrazine	Nafion 117	60	Pt/C (0.5)	148.58	[89]
2021	Sodium borohydride	Nafion 115	50	Pt/C (0.5)	139	[64]
2021	Sodium borohydride	Nafion 212	50	Au-Ni/ MWCNTs	279.5	[34]

Year	Fuel	Membrane	Temp (℃)	Cathode Catalyst (mg cm^{-2})	Peak power density (mW cm^{-2})	Ref.
				(1.0)		
2021	Sodium borohydride	Bipolar interface	25	Pt/C (3.0)	466	90
2022	E-fuel	Nafion 211	60	Pt/C (0.5)	1456.0	This work

References

1. F. Ueckerdt, C. Bauer, A. Dirnaichner, J. Everall, R. Sacchi and G. Luderer, *Nature Climate Change*, 2021, **11**, 384-393.
2. B. Stolz, M. Held, G. Georges and K. Boulouchos, *Nature Energy*, 2022, 1-10.
3. M. Chen, Y. Zhang, G. Xing, S.-L. Chou and Y. Tang, *Energy & Environmental Science*, 2021, **14**, 3323-3351.
4. O. C. Esan, X. Shi, Z. Pan, X. Huo, L. An and T. Zhao, *Advanced Energy Materials*, 2020, **10**, 2000758.
5. H. Feng, D. Liu, Y. Zhang, X. Shi, O. C. Esan, Q. Li, R. Chen and L. An, *Advanced Energy Materials*, 2022, 2200469.
6. S. Chen, M. Zhang, P. Zou, B. Sun and S. Tao, *Energy & Environmental Science*, 2022.
7. A. Sajid, E. Pervaiz, H. Ali, T. Noor and M. M. Baig, *International Journal of Energy Research*, 2022, **46**, 6953-6988.
8. N. Shaari, S. K. Kamarudin, R. Bahru, S. H. Osman and N. A. I. Md Ishak, *International Journal of Energy Research*, 2021, **45**, 6644-6688.
9. D. A. Cullen, K. C. Neyerlin, R. K. Ahluwalia, R. Mukundan, K. L. More, R. L. Borup, A. Z. Weber, D. J. Myers and A. Kusoglu, *Nature energy*, 2021, **6**, 462-474.
10. K. Swider-Lyons and D. Deitz, *ECS Transactions*, 2016, **75**, 479.
11. V. S. Pinheiro, F. M. Souza, T. C. Gentil, A. N. Nascimento, L. S. Parreira, M. I. Sairre, B. L. Batista and M. C. Santos, *Journal of Alloys and Compounds*, 2022, **899**, 163361.
12. Y. Yang, X. Zhu, Q. Wang, D. Ye, R. Chen and Q. Liao, *Applied Thermal Engineering*, 2022, **203**, 117937.
13. H. Jiang, L. Wei, X. Fan, J. Xu, W. Shyy and T. Zhao, *J Science Bulletin*, 2019, **64**, 270-280.
14. X. Shi, X. Huo, O. C. Esan, Y. Ma, L. An and T. Zhao, *Journal of Power Sources*, 2021, **506**, 230198.
15. X. Shi, X. Huo, O. C. Esan, Y. Dai, L. An and T. Zhao, *ACS Applied Materials & Interfaces*, 2022, **14**, 18600-18606.
16. X. Shi, X. Huo, O. C. Esan, L. An and T. Zhao, *Applied Energy*, 2021, **297**, 117145.
17. X. Shi, Y. Dai, O. C. Esan, X. Huo, L. An and T. Zhao, *ACS Applied Materials & Interfaces*, 2021, **13**, 48795-48800.
18. O. C. Esan, X. Shi, Y. Dai, L. An and T. S. Zhao, *Applied Energy*, 2022, **311**, 118677.
19. S. Fukuzumi, Y.-M. Lee and W. Nam, *Chinese Journal of Catalysis*, 2021, **42**, 1241-1252.
20. S. J. Lao, H. Y. Qin, L. Q. Ye, B. H. Liu and Z. P. Li, *Journal of Power Sources*, 2010, **195**, 4135-4138.
21. T. H. Oh, *Aerospace Science and Technology*, 2016, **58**, 511-517.
22. N. Luo, G. Miley, K.-J. Kim, R. Burton and X. Huang, *Journal of Power Sources*, 2008, **185**, 685-690.
23. L. An, T. Zhao, X. Yan, X. Zhou and P. Tan, *Science Bulletin*, 2015, **60**, 55-64.

24. G. H. Miley, N. Luo, J. Mather, R. Burton, G. Hawkins, L. Gu, E. Byrd, R. Gimlin, P. J. Shrestha and G. Benavides, *Journal of Power Sources*, 2007, **165**, 509-516.
25. R. O. Stroman, G. S. Jackson, Y. Garsany and K. Swider-Lyons, *Journal of Power Sources*, 2014, **271**, 421-430.
26. X. Jing, D. Cao, Y. Liu, G. Wang, J. Yin, Q. Wen and Y. Gao, *Journal of electroanalytical chemistry*, 2011, **658**, 46-51.
27. A. Oshchepkov, A. Bonnefont, G. Maranzana, E. R. Savinova and M. Chatenet, *Current Opinion in Electrochemistry*, 2022, **32**, 100883.
28. Z. Pan, Z. Zhang, A. Tahir, O. C. Esan, X. Liu, H. Wang and L. An, *International Journal of Energy Research*, 2022, **46**, 13820-13831.
29. R. M. Hjelm, C. Lafforgue, R. W. Atkinson, Y. Garsany, R. O. Stroman, M. Chatenet and K. Swider-Lyons, *Journal of The Electrochemical Society*, 2019, **166**, F1218.
30. K. Swider-Lyons, R. M. Hjelm, Y. Garsany, C. Lafforgue and M. Chatenet, *Journal of The Electrochemical Society*, 2020, **167**, 164508.
31. R. M. E. Hjelm, Y. Garsany, R. W. Atkinson, R. O. N. Stroman, K. Swider-Lyons, C. Lafforgue and M. Chatenet, *ECS Transactions*, 2017, **80**, 1033.
32. P.-Y. Olu, N. Job and M. Chatenet, *Journal of Power Sources*, 2016, **327**, 235-257.
33. C. P. de León, F. Walsh, C. Patrissi, M. Medeiros, R. Bessette, R. Reeve, J. Lakeman, A. Rose and D. Browning, *Electrochemistry communications*, 2008, **10**, 1610-1613.
34. T. H. Oh, *Renewable Energy*, 2021, **163**, 930-938.
35. S. S. Yu, T. H. Lee and T. H. Oh, *Fuel*, 2022, **315**, 123151.
36. Z. Wang, J. Parrondo, C. He, S. Sankarasubramanian and V. Ramani, *Nature Energy*, 2019, **4**, 281-289.
37. C. G. Arges, V. Prabhakaran, L. Wang and V. Ramani, *International Journal of Hydrogen Energy*, 2014, **39**, 14312-14321.
38. Z. Wang, S. Sankarasubramanian and V. Ramani, *Current Opinion in Electrochemistry*, 2018, **12**, 240-245.
39. M. Chatenet, *Nature Energy*, 2019, **4**, 261-262.
40. O. C. Esan, X. Shi, X. Su, Y. Dai, L. An and T. Zhao, *Journal of Power Sources*, 2021, **501**, 230023.
41. Z. Pan, B. Huang and L. An, *International Journal of Energy Research*, 2019, **43**, 2583-2591.
42. B. Jiang, L. Wu, L. Yu, X. Qiu and J. Xi, *Journal of Membrane Science*, 2016, **510**, 18-26.
43. L. An and T. Zhao, *International journal of hydrogen energy*, 2011, **36**, 9994-9999.
44. H. Jiang, W. Shyy, M. Wu, L. Wei and T. Zhao, *Journal of Power Sources*, 2017, **365**, 34-42.
45. Z. Wang, S. Sankarasubramanian and V. Ramani, *Cell Reports Physical Science*, 2020, **1**, 100084.
46. J. Ma and Y. Sahai, *ECS Transactions*, 2012, **42**, 101.
47. G. H. Miley, R. Bernas, K.-J. Kim and N. Luo, *ECS Transactions*, 2009, **17**, 525.

48. Y. Li, Y. He and W. Yang, *Journal of Power Sources*, 2015, **278**, 569-573.
49. L. An, T. Zhao, R. Chen and Q. Wu, *Journal of power sources*, 2011, **196**, 6219-6222.
50. T. H. Oh, *Renewable Energy*, 2021, **178**, 1156-1164.
51. Z. Pan, Y. Bi and L. An, *Applied Energy*, 2019, **250**, 846-854.
52. Z. Pan, H. Zhuang, Y. Bi and L. An, *Journal of Power Sources*, 2019, **437**, 226944.
53. L. An, T. S. Zhao and J. B. Xu, *International Journal of Hydrogen Energy*, 2011, **36**, 13089-13095.
54. R. Raman and A. Shukla, *Journal of applied electrochemistry*, 2005, **35**, 1157-1161.
55. X. Shi, X. Huo, Y. Ma, Z. Pan and L. An, *Cell Reports Physical Science*, 2020, **1**, 100102.
56. Y. Zhao, L. Liu, X. Qiu and J. Xi, *Electrochimica Acta*, 2019, **303**, 21-31.
57. X. Shi, O. C. Esan, X. Huo, Y. Ma, Z. Pan, L. An and T. Zhao, *Progress in Energy and Combustion Science*, 2021, **85**, 100926.
58. X. Shi, Y. Bi, O. C. Esan and L. An, in *60 Years of the Loeb-Sourirajan Membrane*, Elsevier, 2022, pp. 155-175.
59. X. Shi, Y. Ma, X. Huo, O. C. Esan and L. An, *International Journal of Green Energy*, 2021, 1-7.
60. L. An and C. Jung, *Applied energy*, 2017, **205**, 1270-1282.
61. S. Won, K. Oh and H. Ju, *Electrochimica Acta*, 2015, **177**, 310-320.
62. W. Haijun, W. Cheng, L. Zhixiang and M. Zongqiang, *International journal of hydrogen energy*, 2010, **35**, 2648-2651.
63. Y. Li, H. Wu, Y. He, Y. Liu and L. Jin, *Journal of Power Sources*, 2015, **287**, 75-80.
64. A. Uzundurukan, E. S. Akça, Y. Budak and Y. Devrim, *Renewable Energy*, 2021, **172**, 1351-1364.
65. L. An, T. S. Zhao, L. Zeng and X. H. Yan, *International Journal of Hydrogen Energy*, 2014, **39**, 2320-2324.
66. L. An, T. Zhao, X. Zhou, L. Wei and X. Yan, *RSC Advances*, 2014, **4**, 65031-65034.
67. R. K. Raman, N. A. Choudhury and A. K. Shukla, *Electrochemical and Solid-State Letters*, 2004, **7**, A488.
68. N. Choudhury, R. Raman, S. Sampath and A. Shukla, *Journal of Power Sources*, 2005, **143**, 1-8.
69. S. Towne, M. Carella, W. Mustain, V. Viswanathan, P. Rieke, U. Pasaogullari and P. Singh, *ECS Transactions*, 2009, **25**, 1951.
70. D. Santos and C. Sequeira, *Journal of The Electrochemical Society*, 2009, **157**, B13.
71. J. Ma, Y. Sahai and R. G. Buchheit, *Journal of Power Sources*, 2010, **195**, 4709-4713.
72. L. An, T. S. Zhao, R. Chen and Q. X. Wu, *Journal of Power Sources*, 2011, **196**, 6219-6222.
73. L. An and T. S. Zhao, *International Journal of Hydrogen Energy*, 2011, **36**, 9994-9999.

74. N. A. Choudhury, J. Ma, Y. Sahai and R. G. Buchheit, *Journal of Power Sources*, 2011, **196**, 5817-5822.
75. X. Yan, F. Meng, Y. Xie, J. Liu and Y. Ding, *Scientific reports*, 2012, **2**, 1-7.
76. A. Déctor, J. P. Esquivel, M. J. González, M. Guerra-Balcázar, J. Ledesma-García, N. Sabaté and L. G. Arriaga, *Electrochimica Acta*, 2013, **92**, 31-35.
77. W. Jin, J. Liu, Y. Wang, Y. Yao, J. Gu and Z. Zou, *International journal of hydrogen energy*, 2013, **38**, 10992-10997.
78. L. Yi, W. Wei, C. Zhao, C. Yang, L. Tian, J. Liu and X. Wang, *Electrochimica Acta*, 2015, **158**, 209-218.
79. X. H. Yan, T. S. Zhao, L. An, G. Zhao and L. Shi, *International Journal of Hydrogen Energy*, 2016, **41**, 5135-5140.
80. Y. Li, *International Journal of Hydrogen Energy*, 2016, **41**, 3600-3604.
81. M. Abdolmaleki, I. Ahadzadeh and H. Goudarziafshar, *International Journal of Hydrogen Energy*, 2017, **42**, 15623-15631.
82. M. G. Hosseini, R. Mahmoodi and M. Abdolmaleki, *New Journal of Chemistry*, 2018, **42**, 12222-12233.
83. K. Swider-Lyons, Y. Garsany and R. Hjelm, 2019.
84. Z. Pan, Y. Bi and L. An, *Applied Energy*, 2020, **258**, 114060.
85. G. Braesch, Z. Wang, S. Sankarasubramanian, A. G. Oshchepkov, A. Bonnefont, E. R. Savinova, V. Ramani and M. Chatenet, *Journal of Materials Chemistry A*, 2020, **8**, 20543-20552.
86. B. Lu, W. Yuan, X. Su, Z. Zhuang, Y. Ke and Y. Tang, *Energy Technology*, 2020, **8**, 1901360.
87. Z. Wang, M. Mandal, S. Sankarasubramanian, G. Huang, P. A. Kohl and V. K. Ramani, *ACS Applied Energy Materials*, 2020, **3**, 4449-4456.
88. M. G. Hosseini, V. Daneshvari-Esfahlan, H. Aghajani, S. Wolf and V. Hacker, *Catalysts*, 2021, **11**, 1372.
89. M. G. Hosseini, V. Daneshvari-Esfahlan, S. Wolf and V. Hacker, *RSC Advances*, 2021, **11**, 39223-39232.
90. S. Saha, P. Gayen, Z. Wang, R. J. Dixit, K. Sharma, S. Basu and V. K. Ramani, *ACS Catalysis*, 2021, **11**, 8417-8430.

Highlights

- An e-fuel/hydrogen peroxide fuel cell is proposed.
- The fuel cell exhibits a peak power density of 1456.0 mW cm^{-2} at 60 ℃.
- Effects of various operating conditions on the cell performance are investigated.
- The cell demonstrates its promising applications for high-power systems.